A&A 625, A133 (2019)
https://doi.org/10.1051/0004-6361/201834902

Astronomy & Astrophysics

Spectroscopic and dynamical properties of comet C/2018 F4, likely a true average former member of the Oort cloud⋆

J. Licandro[1,2], C. de la Fuente Marcos[3], R. de la Fuente Marcos[4], J. de León[1,2], M. Serra-Ricart[1,2], and A. Cabrera-Lavers[5,1,2]

[1] Instituto de Astrofísica de Canarias (IAC), C/ Vía Láctea s/n, 38205 La Laguna, Tenerife, Spain
e-mail: jlicandr@iac.es
[2] Departamento de Astrofísica, Universidad de La Laguna, 38206 La Laguna, Tenerife, Spain
[3] Universidad Complutense de Madrid, Ciudad Universitaria, 28040 Madrid, Spain
[4] AEGORA Research Group, Facultad de Ciencias Matemáticas, Universidad Complutense de Madrid, Ciudad Universitaria, 28040 Madrid, Spain
[5] GRANTECAN, Cuesta de San José s/n, 38712 Breña Baja, La Palma, Spain

Received 17 December 2018 / Accepted 15 March 2019

ABSTRACT

Context. The population of comets hosted by the Oort cloud is heterogeneous. Most studies in this area have focused on highly active objects, those with small perihelion distances or examples of objects with peculiar physical properties and/or unusual chemical compositions. This may have produced a biased sample of Oort cloud comets in which the most common objects may be rare, particularly those with perihelia well beyond the orbit of the Earth. Within this context, the known Oort cloud comets may not be representative of the full sample meaning that our current knowledge of the appearance of the average Oort cloud comet may not be accurate. Comet C/2018 F4 (PANSTARRS) is an object of interest in this regard.
Aims. Here, we study the spectral properties in the visible region and the cometary activity of C/2018 F4, and we also explore its orbital evolution with the aim of understanding its origin within the context of known minor bodies moving along nearly parabolic or hyperbolic paths.
Methods. We present observations obtained with the 10.4 m Gran Telescopio Canarias (GTC) that we use to derive the spectral class and visible slope of C/2018 F4 as well as to characterise its level of cometary activity. Direct N-body simulations are carried out to explore its orbital evolution.
Results. The absolute magnitude of C/2018 F4 is $H_r > 13.62 \pm 0.04$ which puts a strong limit on its diameter, $D < 10.4$ km, assuming a $p_V = 0.04$ cometary-like value of the albedo. The object presents a conspicuous coma, with a level of activity comparable to those of other comets observed at similar heliocentric distances. Comet C/2018 F4 has a visible spectrum consistent with that of an X-type asteroid, and has a spectral slope $S' = 4.0 \pm 1.0\%/1000$ Å and no evidence of hydration. The spectrum matches those of well-studied primitive asteroids and comets. The analysis of its dynamical evolution prior to discovery suggests that C/2018 F4 is not of extrasolar origin.
Conclusions. Although the present-day heliocentric orbit of C/2018 F4 is slightly hyperbolic, both its observational properties and past orbital evolution are consistent with those of a typical dynamically old comet with an origin in the Oort cloud.

Key words. comets: individual: C/2018 F4 – comets: general – Oort cloud – techniques: spectroscopic – techniques: photometric – methods: numerical

1. Introduction

In our solar system, a number of populations of small bodies are well studied and the notion of an average or typical member of such populations is well defined; good examples are the near-Earth objects (NEOs; see e.g. Granvik et al. 2018) or the Jupiter-family comets (see e.g. Fernández et al. 1999; Snodgrass et al. 2011). Unfortunately, the appearance of an average Oort cloud comet remains unclear and this could be the result of most studies focusing on the extreme cases.

The Oort cloud (Oort 1950) is a spherical structure that surrounds the solar system with an outer boundary located beyond 50 000 to 200 000 AU. The Oort cloud hosts a population of comets of heterogeneous nature (see e.g. Stern & Weissman 2001; Gibb et al. 2003; Fernández et al. 2004; Meech et al. 2016; Bauer et al. 2017). Most authors consider the Oort cloud to have appeared very early in the history of the solar system, nearly 4.6 Gyr ago, and to be made of fossil debris from the primordial protoplanetary disc. Importantly, the solar system was born within a star cluster (see e.g. Kaib & Quinn 2008). Based on this information, Levison et al. (2010) suggest that perhaps over 90% of the material currently present in the Oort cloud is of extrasolar origin, having been captured from the protoplanetary discs of other stars when the Sun was still part of the open star cluster or stellar association where it was born. An analysis of a sufficiently representative sample of objects from the Oort cloud should be able to either confirm or reject a dominant primordial extrasolar origin for the populations of small bodies hosted by the

⋆ Based on observations made with the GTC telescope, in the Spanish Observatorio del Roque de los Muchachos of the Instituto de Astrofísica de Canarias, under Director's Discretionary Time (program ID GTC2018-096).

Table 1. Heliocentric and barycentric orbital elements and 1σ uncertainties of comet C/2018 F4 (PANSTARRS).

Orbital parameter		Heliocentric	Barycentric
Perihelion distance, q (AU)	=	3.4417 ± 0.0004	3.4355
Eccentricity, e	=	1.00077 ± 0.00011	0.99771
Inclination, i (°)	=	78.160 ± 0.003	78.256
Longitude of the ascending node, Ω (°)	=	26.51923 ± 0.00004	26.46807
Argument of perihelion, ω (°)	=	263.167 ± 0.004	263.321
Mean anomaly, M (°)	=	-0.0020 ± 0.0004	359.9899

Notes. The orbit determination has been computed at epoch JD 2458227.5 that corresponds to 00:00:00.000 TDB, Barycentric Dynamical Time, on 2018 April 19, J2000.0 ecliptic and equinox. Source: JPL's SSDG SBDB.

Oort cloud. Being able to clearly characterise the appearance of an average Oort cloud member may help in solving this difficult and important problem.

The current sample of known Oort cloud comets is likely biased in favour of relatively active objects, those with short perihelion distances, and those with unusual physical and/or chemical properties; unremarkable comets tend to be missing, perhaps neglected. Among the currently known minor bodies following nearly parabolic or hyperbolic paths – which may have their origin in the Oort cloud – about 75% have data-arcs spanning less than a month and consistently uncertain orbit determinations; only a small subsample has been studied spectroscopically. This suggests that our current perspective on the appearance of the average Oort cloud comet may be inaccurate. Comet C/2018 F4 (PANSTARRS) is an object of interest in this regard.

Comet C/2018 F4 was discovered by the Pan-STARRS survey (Kaiser 2004; Denneau et al. 2013) on 2018 March 17 at 6.4 AU from the Sun and with an apparent magnitude w of 20.4 (Gilmore et al. 2018; S'arneczky et al. 2018; Tichy et al. 2018). It was initially classified as a hyperbolic asteroid, A/2018 F4 (Tichy et al. 2018), and was subsequently reclassified as a comet (S'arneczky et al. 2018). Its current heliocentric orbit determination is based on 185 data points, for an observation arc of 146 days, and it is hyperbolic at the 7σ level, although the barycentric eccentricity is not hyperbolic (see Table 1) at almost the 21σ level; σ levels have been computed using the formal uncertainty on the eccentricity in Table 1. Its trajectory is approximately perpendicular to the plane of the solar system with the descending node being at about 6 AU from the Sun and the ascending node being far from any planetary path, stranded approximately midway between the orbits of Jupiter and Saturn.

The aim of the research presented here is two-fold: (1) we aim to study the activity and surface properties of C/2018 F4 by obtaining a high-S/N image and a low-resolution spectrum in the visible, and to compare them to the activity and spectral properties observed in other comets (see e.g. Licandro et al. 2018); and (2) to explore its dynamics in order to determine whether it is an Oort cloud comet, old or new, or perhaps an interstellar interloper. The paper is organised as follows. In Sect. 2, observations, data reduction, and spectral extraction are described. In Sect. 3, we analyse the observed coma and the spectral properties of the comet, and compare them to those of other comets. In Sect. 4, we explore the dynamical evolution of C/2018 F4 before finally presenting our conclusions in Sect. 5.

2. Observations

Images and low-resolution visible spectra of C/2018 F4 (PANSTARRS) were obtained in service mode on 2018 April 12 using the Optical System for Imaging and Low Resolution Integrated Spectroscopy (OSIRIS) camera spectrograph (Cepa et al. 2000; Cepa 2010) at the 10.4 m Gran Telescopio Canarias (GTC). Two images, one with an exposure time of 180 s and the other of 30 s, were obtained between 0:33 and 0:43 UTC (at an airmass of 1.32) using the SLOAN r' filter. Three spectra, each one with an exposure time of 900 s, were obtained between 0:48 and 1:32 UTC (at an airmass of 1.29). OSIRIS has a mosaic of two Marconi 2048×4096 pixel CCD detectors, with a total unvignetted field of view of 7.8×7.8 arcminutes, and a plate scale of 0.127″/px. In order to increase the S/N, we selected the 2×2 binning and the standard operation mode with a readout speed of 200 kHz (with a gain of 0.95 e−/ADU and a readout noise of 4.5 e−). The tracking of the telescope matched the proper motion of the object during the observations. We found C/2018 F4 to be at 6.23 and 5.23 AU, heliocentric and geocentric distances, respectively, and its phase angle was $\alpha = 0\overset{\circ}{.}9$ at the time of the observations.

The spectra were obtained using the R300R grism in combination with a second-order spectral filter that produces a spectrum in the range 4800–9000 Å with a dispersion of 32.25 Å/px for the used 2.5″ slit width. The slit was oriented in parallactic angle to account for possible variable seeing conditions and to minimise losses due to atmospheric dispersion. The three consecutive spectra were shifted in the slit direction by 10″ to better correct for fringing. In addition, two G2V stars – SA102-1081 and SA107-998 – from the Landolt catalogue (Landolt 1992) were observed immediately before and after the object, and at similar airmass (1.26 and 1.27, respectively) using the same spectral configuration. These stars are used as solar analogues to correct for telluric absorptions and to obtain relative reflectance spectra.

Data reduction was carried out using standard Image Reduction and Analysis Facility (IRAF[1]) procedures. The r' images obtained were over-scan and bias corrected, flat-field corrected using sky-flats, and flux calibrated using standard stars observed the same night. The 180 s image is shown in Fig. 1. Spectral images were over-scan and bias corrected, and then flat-field corrected using lamp flats. The 2D spectra were extracted, sky background subtracted, and collapsed to one dimension. The wavelength calibration was done using Xe + Ne + HgAr lamps. Finally, the three spectra of the object were averaged to obtain the final spectrum. As pointed out above, two G2V stars were observed under the same conditions in order to improve the quality of the final comet reflectance spectra and to minimise potential variations in spectral slope introduced by the use of just one star. The averaged spectrum of the object was divided by that of each G2V star, and the resulting spectra were normalized to unity at 0.55 μm to obtain the reflectance spectrum. The final reflectance spectrum of C/2018 F4, binned to a resolution of 50 Å, is shown in Fig. 2.

3. Results and analysis

In this section, we first analyse the images of C/2018 F4 (PANSTARRS) – the deepest is shown in Fig. 1 – to look for signs of comet-like activity, and measure the nuclear magnitude and activity levels. We then analyse its spectral properties, derive its taxonomical classification, and compute its visible spectral

[1] IRAF is distributed by the National Optical Astronomy Observatory, which is operated by the Association of Universities for Research in Astronomy, Inc., under cooperative agreement with the National Science Foundation.

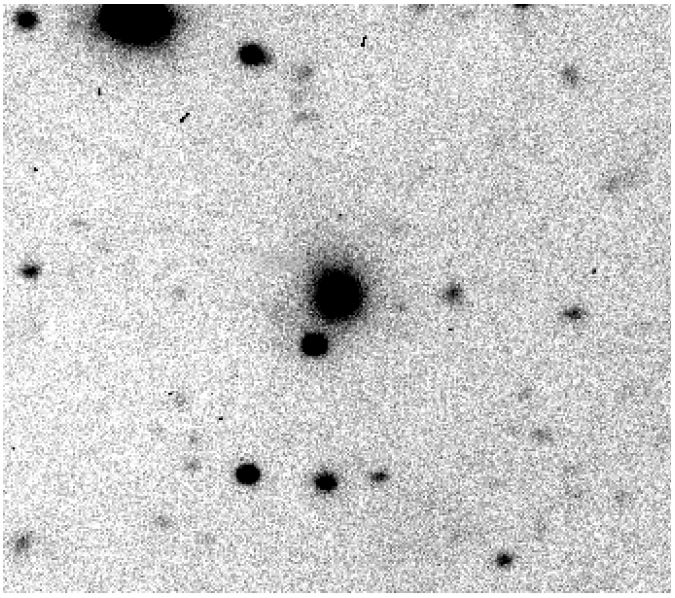

Fig. 1. Image of C/2018 F4 (PANSTARRS) obtained on 2018 April 12. The image is a $90 \times 90''$ field; north is up, east to the left. The object is found at the centre of the image and presents a faint coma indicative of some modest comet-like activity.

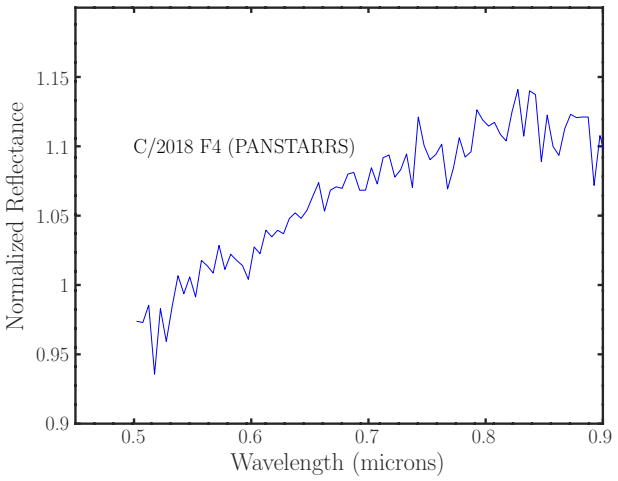

Fig. 2. Visible reflectance spectrum of C/2018 F4 (PANSTARRS), normalized to unity at 0.55 μm.

slope. Following the procedure described by De Prá et al. (2018), we also look for the typical 0.7 μm absorption band associated with the presence of hydrated minerals and observed on the surface of some primitive asteroids. We finally compare these spectral properties to those of known comet nuclei and dormant comets.

3.1. Comet C/2018 F4 observed activity

Comet C/2018 F4 presents a rather obvious and compact faint coma as seen in Fig. 1. The radial profiles of the comet and a field star shown in Fig. 3 clearly indicate that the point spread function (PSF) of the comet is wider (with an $FWHM = 6.4$ pixels) than that of the field stars ($FWHM = 4.2$ pixels). In order to assess the relative contributions of the nucleus and coma to the observed radial profile of the comet, we performed a simple analysis assuming an isotropic dust coma with surface

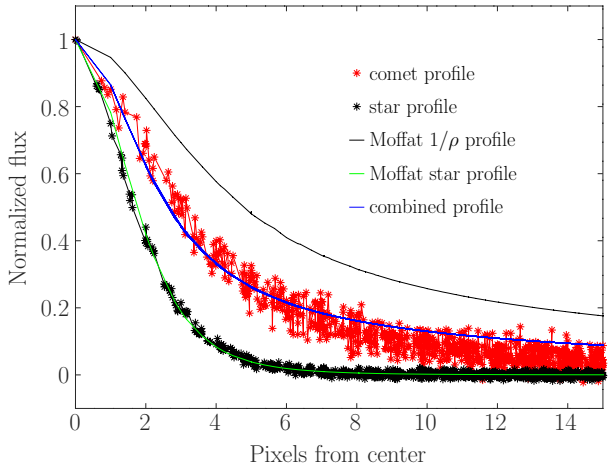

Fig. 3. Normalized radial profile of C/2018 F4 (PANSTARRS) in the image shown in Fig. 1 (in red) compared to that of a field star (in black). The Moffat profile of a point-like source (solid line in green) with the FWHM of the stars in the images, and the corresponding profile of an extended object (solid line in black) with a $1/\rho$ profile (the profile of an isotropic dust coma) are shown. The solid line in blue is the 50:50 linear combination of the point-like source (nucleus) and $1/\rho$ profile (dust coma). The similarity of the combined profile to the observed one suggests that the nucleus contributes significantly to the overall brightness of the comet.

brightness inversely proportional to the projected cometocentric distance (ρ). Using the IRAF task MKOBJECT, we created a synthetic image with two objects: (1) a point-like source and (2) an extended object with a $1/\rho$ profile. We assumed a Moffat PSF with the value of the FWHM measured for the field stars in the image of the comet. The radial profiles of these objects are also shown in Fig. 3. We note that the point-like source (labelled as Moffat star profile) fits the profile of the stars in the comet image very well, while the $1/\rho$ profile (labelled as Moffat $1/\rho$ profile) does not fit that of the comet at all. A 50:50 linear combination of the star and $1/\rho$ profiles matches the observed profile of the comet reasonably well, which strongly suggests that the contribution of the nucleus to the total brightness close to the optocentre of the comet is indeed significant.

The apparent magnitude of the comet was measured using several apertures: $r' = 21.22 \pm 0.04$ (6 pixels), $r' = 19.90 \pm 0.04$ (12 pixels), and $r' = 19.47 \pm 0.04$ (18 pixels). The brightness of the comet greatly increases by 1.75 magnitudes when moving from 18 to 6 pixel apertures. On the other hand, the magnitude variation between these two apertures computed for the field stars is only of 0.20. Such a difference is due to the contribution of the observed coma. This clearly shows that the brightness of the comet nucleus, even using the small 6 pixel aperture, is strongly contaminated by the coma as we also showed in the analysis of the profiles. An apparent magnitude $r' = 21.22 \pm 0.04$ is simply a lower limit for the value of the nuclear magnitude of C/2018 F4, which in turn puts a robust limit to the nuclear magnitude and the size of the comet. In the combined profile described above, the coma contribution is 3.7 times larger than that of the nucleus, and thus the nuclear magnitude could be ~1.4 magnitudes fainter. From the apparent magnitude, we derived an absolute nuclear magnitude of $H_r > 13.62 \pm 0.04$ using the procedure described in Licandro et al. (2000). Considering the solar colour transformations, the absolute magnitude in the visible is $H_V > 14.02 \pm 0.04$, and assuming an albedo of $p_V = 0.04$, typical of comet nuclei (see Licandro et al. 2018), this absolute

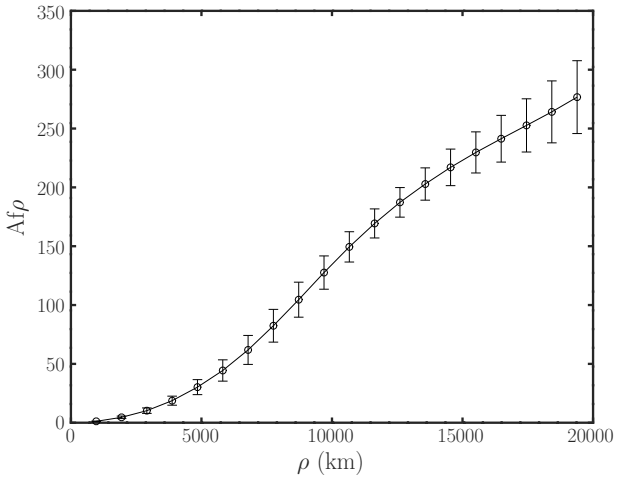

Fig. 4. Variation of $Af\rho$ with ρ.

magnitude limit corresponds to a diameter of $D < 10.4$ km for comet C/2018 F4.

In order to evaluate the overall level of cometary activity (i.e. dust production rate) present during the observations, we computed the $Af\rho$ parameter – or product between the albedo, the filling factor, and the radius of the coma (Ahearn et al. 1984) – for different cometocentric distances (ρ) as shown in Fig. 4. At $\rho = 10\,000$ km, $Af\rho = 148 \pm 13$ cm. Within the context of comet-like activity at large heliocentric distances, this value of $Af\rho$ agrees well with those of P/2008 CL94 (Lemmon) and P/2011 S1 (Gibbs), of 106 ± 3 cm and 76 ± 8 cm, respectively (Kulyk et al. 2016) and it is slightly below the mean $Af\rho$ value reported for comets observed at similar heliocentric distances by Mazzotta Epifani et al. (2014), but still compatible with the less-active comets reported in this paper. The existence of comet-like activity beyond the zone of water-ice sublimation is very well known, and our results show that C/2018 F4 behaves in a similar manner to other comets observed at similar heliocentric distances.

3.2. C/2018 F4 spectral properties

A spectral slope of $S' = 4.0 \pm 1.0\%/1000$ Å is computed for the spectrum of C/2018 F4 following the S' definition in Luu & Jewitt (1996), and considering the 0.55–0.86 μm wavelength range (where the observed reflectance is well represented by a linear fit). The spectrum is normalized to unity at 0.55 μm. The quoted uncertainty in the value of S' has been computed as the standard deviation (σ) of the S' values obtained for each single reflectance spectrum of the object; that is, the reflectance spectrum obtained for each single 900 s exposure time spectrum of the object and each single spectrum of the G2V stars obtained during the night when the observations were completed. The derived uncertainty (~1.0%/1000 Å) is compatible with the values (1–0.5%/1000 Å) usually obtained under good observational conditions, when several solar analogue stars have been observed. We adopt this value as the error of the computed slope instead of using the error obtained from the linear fit, which is much smaller. Using the online tool for modelling the spectra of asteroids, M4AST[2] (Popescu et al. 2012), we obtained the taxonomical classification of C/2018 F4. Its spectrum corresponds to that of an X-type asteroid (Clark et al. 2004; Fornasier et al. 2011). As described by Popescu et al. (2012), M4AST first applies a polynomial fit to the asteroid spectrum, with varying order, and then compares this fit at the corresponding wavelengths to templates of each taxonomical class defined by Bus & Binzel (2002) taxonomy. It then selects the taxonomic class with the smallest chi-squared value.

Only a few visible or near-infrared spectra of comet nuclei have been published, but all of them are featureless with a red slope in the 0.5–2.5 μm region, typical of X- or D-type asteroids and similar to the spectrum of C/2018 F4 presented here (see Licandro et al. 2018 and references therein). The photometric colours of comets are also typical of X- or D-type asteroids (see e.g. Jewitt 2015).

The presence of aqueously altered minerals on asteroid surfaces can be inferred by a shallow spectral absorption band centred at 0.7 μm. No signatures of this feature are present in the spectrum of C/2018 F4 (see Fig. 2). In any case, the absence of this feature does not mean that there are no hydrated minerals on the surface of the object. Several asteroids with hydrated minerals on their surfaces, inferred by a strong absorption feature in the 3-μm region, do not present the 0.7 μm band. In contrast, whenever the 0.7 μm band is present, the 3 μm band is also observed (see e.g. Howell et al. 2011; Rivkin et al. 2015). The lack of evidence of water hydration on the surface of C/2018 F4 from its visible spectrum is also compatible with a cometary origin. Comet 67P/Churyumov–Gerasimenko is devoid of hydrated minerals (Bardyn et al. 2017) and the visible spectra of cometary nuclei do not present the features produced by hydrated minerals: the band centred at 0.7 μm and that at 0.5 μm. In particular, the visible spectrum of C/2018 F4 is different from those of the so-called Manx comets, long-period comets displaying only residual activity even at small perihelion distances (Meech et al. 2016), as no significant dip beyond 0.75 μm is observed.

The results presented above should be taken with some caution, since the observed spectrum of C/2018 F4 is not exactly that of the comet nucleus; there is an important contribution of the coma (~60% of the flux in the slit corresponds to scattered light from the coma according to the profile analysis presented above). In terms of slope determination and spectral classification, this should not affect our conclusions given the fact that the colour of the comet coma is similar to that of the nucleus (see Jewitt 2015). In contrast, such a contribution could have masked the presence of a weak absorption band like the 0.7 μm one due to aqueously altered minerals.

4. Dynamics

Aiming at exploring the dynamical evolution of C/2018 F4 (PANSTARRS), we have used data – heliocentric and barycentric orbital elements and their uncertainties – provided by Jet Propulsion Laboratory's Solar System Dynamics Group Small-Body Database (JPL's SSDG SBDB, Giorgini 2015)[3]. Here, the full N-body calculations required to investigate the pre- and post-perihelion trajectories of this and other objects have been carried out as described by de la Fuente Marcos & de la Fuente Marcos (2012) and do not include non-gravitational forces. The orbit determination in Table 1 did not require non-gravitational terms to fit the available astrometry; therefore, any contribution due to asymmetric outgassing is probably a second-order effect. Neglecting the role of non-gravitational forces in this case is unlikely to have any major impact on our conclusions. When nominal orbits are not used, the Cartesian state vectors are generated by applying the Monte Carlo using the Covariance Matrix

[2] http://m4ast.imcce.fr/

[3] https://ssd.jpl.nasa.gov/sbdb.cgi

method described by de la Fuente Marcos & de la Fuente Marcos (2015) and modified here to make it work with hyperbolic orbits; the covariance matrices necessary to generate initial positions and velocities have been obtained from JPL's HORIZONS[4], which is also the source of other input data required to perform the calculations such as barycentric Cartesian state vectors for planets and other solar system bodies. This approach has previously been used to independently confirm that C/2017 K2 (PANSTARRS) is a bound and dynamically old Oort cloud comet (de la Fuente Marcos & de la Fuente Marcos 2018).

The analysis of the pre-perihelion trajectory of C/2018 F4 might shed some light on its true origin because although its present-day heliocentric orbital determination is nominally hyperbolic (see Table 1), it may or may not have followed an elliptical path in the past; realistic N-body simulations can help in investigating this critical issue. We have performed integrations backward in time of 1024 control orbits of this object; our physical model includes the perturbations by the eight major planets, the Moon, the barycentre of the Pluto–Charon system, and the three largest asteroids. A statistical analysis of the results indicates that about 38% of the control orbits are compatible with the object coming from the interstellar medium at low relative velocity with respect to the Sun. For this hyperbolic subsample and 1 Myr into the past, the average distance to the comet from the Sun was 0.3 ± 0.2 pc (or 60 855 AU), moving inwards at -0.5 ± 0.4 km s^{-1} and projected towards $\alpha = 16^{\rm h}\ 59^{\rm m}\ 12^{\rm s}$ and $\delta = +75^\circ\ 18'\ 10''$ ($255^\circ \pm 13^\circ, +75^\circ \pm 2^\circ$) in the constellation of Ursa Minor (geocentric radiant or antapex) with Galactic coordinates $l = 107\overset{\circ}{.}41$, $b = +33\overset{\circ}{.}18$, and ecliptic coordinates $\lambda = 112\overset{\circ}{.}56$, $\beta = +80\overset{\circ}{.}02$, thus well separated from the ecliptic and the Galactic disc. The study of its post-perihelion trajectory requires the analysis of a similar set of N-body simulations, but forward in time; it will reach perihelion on 2019 December 4. Out of 1024 control orbits and after 1 Myr of simulated time, we observe that nearly 51% lead the then unbound object towards interstellar space.

In order to better understand the past, present, and future orbital evolution of C/2018 F4 within the context of other objects with similar osculating orbital elements, we have searched JPL's SSDG SBDB and found that the heliocentric orbit determination in Table 1 is somewhat similar in terms of perihelion distance, q, and inclination, i, to those of the long-period comets C/1997 BA6 (Spacewatch), $q = 3.436$ AU, $e = 0.999$, $i = 72\overset{\circ}{.}7$, and C/2007 M2 (Catalina), $q = 3.541$ AU, $e = 0.999$, $i = 80\overset{\circ}{.}9$, but also to those of the slightly hyperbolic comets C/1987 W3 (Jensen–Shoemaker), $q = 3.333$ AU, $e = 1.005$ (its barycentric eccentricity is also slightly hyperbolic, 1.000053), $i = 76\overset{\circ}{.}7$, and C/2000 SV74 (LINEAR), $q = 3.542$ AU, $e = 1.005$ (as in the case of C/2018 F4, its barycentric eccentricity is not hyperbolic, 0.99994), $i = 75\overset{\circ}{.}2$. In principle, these objects have not been selected to argue for some sort of physical or dynamical association with C/2018 F4, but to compare orbital evolutions of objects with similar values of q, e, and i. However, it is true that the locations of the orbital poles $((L_{\rm p}, B_{\rm p}) = (\Omega - 90^\circ, 90^\circ - i)$; see for example Murray & Dermott 1999) of C/2000 SV74 and C/2018 F4 are close in the sky, ($294\overset{\circ}{.}2$, $13\overset{\circ}{.}8$) versus ($296\overset{\circ}{.}5$, $11\overset{\circ}{.}8$), respectively. A small angular separation between orbital poles is indicative of a fairly consistent direction of the orbital angular momentum, which suggests that the objects are experiencing a similar background perturbation. In this context, C/2000 SV74 and C/2018 F4 may share the same dynamics even if they are not physically related – their arguments of perihelion are nearly 180° apart.

[4] https://ssd.jpl.nasa.gov/?horizons

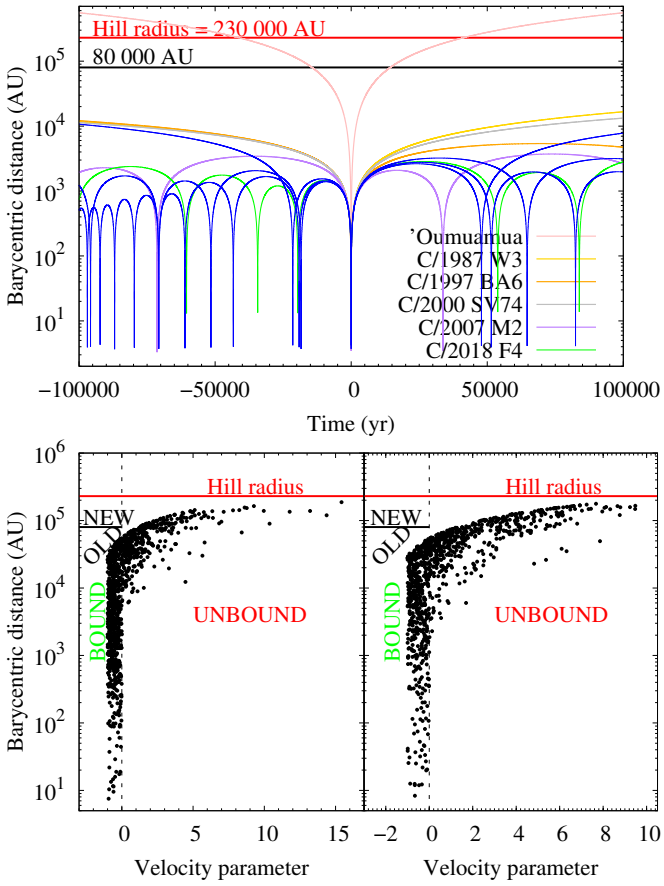

Fig. 5. Evolution of the barycentric distance of 1I/2017 U1 ('Oumuamua), C/1987 W3 (Jensen–Shoemaker), C/1997 BA6 (Spacewatch), C/2000 SV74 (LINEAR), C/2007 M2 (Catalina), C/2018 F4 (PANSTARRS) – all nominal orbits – , and a few representative control orbits of C/2018 F4 (in blue) based on the current orbit determination (*top panel*). The zero instant of time, epoch JDTDB 2458600.5, 27-April-2019, and only the time interval (−100 000, 100 000) yr are displayed. Values of the barycentric distance as a function of the velocity parameter 1 Myr into the past (*left-hand side bottom panel*) and 1 Myr into the future (*right-hand side bottom panel*) for 1024 control orbits of C/2018 F4.

The top panel of Fig. 5 shows the (past and future) short-term orbital evolution of C/2018 F4 (in green, nominal orbit in Table 1) and those of a few representative control orbits (in blue). In addition, we show those of the nominal orbits of 1I/2017 U1 ('Oumuamua), C/1987 W3, C/1997 BA6, C/2000 SV74, and C/2007 M2. The black line marks the aphelion distance – $a\,(1 + e)$, limiting case $e = 1$, semi-major axis, a – that signals the upper boundary of the domain of dynamically old Oort cloud comets (i.e. $a < 40\,000$ AU, see Królikowska & Dybczyński 2017) as opposed to those that may be dynamically new, i.e. bona fide first-time visitors from the Oort cloud; the red line corresponds to the value of the radius of the Hill sphere of the solar system (see e.g. Chebotarev 1965). The bottom panels of Fig. 5 show the barycentric distance as a function of the velocity parameter 1 Myr into the past (left) and into the future (right) for 1024 control orbits of C/2018 F4; the velocity parameter is the difference between the barycentric and escape velocities at the computed barycentric distance in units of the escape velocity. Positive values of the velocity parameter are associated with control orbits that could have been followed by putative visitors from outside the solar system (bottom-left

panel) or that lead to ejections from the solar system (bottom-right panel). In summary, our N-body simulations and statistical analyses suggest that C/2018 F4 may be a dynamically old Oort cloud comet with a probability of 0.62 or, less likely, an interstellar interloper with a probability of 0.38. Given the fact that the inbound velocity may have been as low as 0.5 ± 0.4 km s^{-1}, which is inconsistent with the lower limit for interstellar interlopers determined statistically by de la Fuente Marcos et al. (2018), C/2018 F4 probably originated within the Oort cloud. In addition, C/1987 W3, C/1997 BA6, C/2000 SV74, and C/2007 M2 seem to be dynamically old comets.

5. Conclusions

In this paper, we have present observations of C/2018 F4 (PANSTARRS) obtained with GTC that we have used to derive the spectral class and visible slope of this minor body as well as to characterise its overall level of cometary activity. Direct N-body simulations were carried out to explore its orbital evolution. The object was originally selected to perform this study because early determinations of its orbital elements suggested a possible interstellar origin. Our conclusions can be summarised as follows.

(i) We have determined a lower limit for the absolute magnitude of C/2018 F4, $H_r > 13.62 \pm 0.04$, and an upper limit of the diameter $D < 10.4$ km.

(ii) We show that C/2018 F4 has a visible spectrum consistent with that of an X-type asteroid, with an spectral slope $S' = 4.0 \pm 1.0\%/1000$ Å and no signs of hydrated altered minerals. This is consistent with the spectrum of a comet nucleus.

(iii) We show that the PSF of C/2018 F4 is definitely non-stellar and we confirm the existence of a detectable level of comet-like activity when C/2018 F4 was observed at 6.23 AU from the Sun. We obtained an $Af\rho = 148 \pm 13$ cm measured at $\rho = 10\,000$ km, a value slightly below the mean $Af\rho$ value of comets observed at similar heliocentric distances (Mazzotta Epifani et al. 2014), but still compatible with the level of activity shown by other distant comets.

(iv) The results of the analysis of an extensive set of N-body simulations indicate that the probability of C/2018 F4 being a dynamically old Oort cloud comet is about 62%.

(v) Conversely, the probability of C/2018 F4 having entered the solar system from interstellar space during the past 1 Myr is about 38% with an inbound velocity as low as 0.5 ± 0.4 km s^{-1}, inconsistent with the one expected for a true interstellar interloper.

(vi) The current path followed by C/2018 F4 is unstable, the probability of being ejected out of the solar system during the next 1 Myr is slightly above 50%.

Based on our observational and numerical results, we favour an origin in the solar system for C/2018 F4. C/2018 F4 is likely a true representative of the average Oort cloud comet population.

Acknowledgements. The authors thank the referee A. Fitzsimmons for a constructive and useful report. J.L., M.S.-R., and J.d.L. acknowledge support from the AYA2015-67772-R (MINECO, Spain). J.d.L. acknowledges support from MINECO under the 2015 Severo Ochoa Program SEV-2015-0548. R.d.l.F.M. and C.d.l.F.M. thank S.J. Aarseth for providing the code used in this research and A.I. Gómez de Castro for providing access to computing facilities. This work was partially supported by the Spanish "Ministerio de Economía y Competitividad" (MINECO) under grant ESP2015-68908-R. We made use of the NASA Astrophysics Data System, the ASTRO-PH e-print server, and the MPC data server. Based on observations made with the Gran Telescopio Canarias (GTC) installed in the Spanish Observatorio del Roque de los Muchachos of the Instituto de Astrofísica de Canarias, in the island of La Palma, under Director's Discretionary Time (program ID GTC2018-096).

References

Ahearn, M. F., Schleicher, D. G., Millis, R. L., Feldman, P. D., & Thompson, D. T. 1984, AJ, 89, 579
Bardyn, A., Baklouti, D., Cottin, H., et al. 2017, MNRAS, 469, S712
Bauer, J. M., Grav, T., Fernández, Y. R., et al. 2017, AJ, 154, 53
Bus, S. J., & Binzel, R. P. 2002, Icarus, 158, 146
Cepa, J. 2010, Astrophys. Space Sci. Proc., 14, 15
Cepa, J., Aguiar, M., Escalera, V. G., et al. 2000, in Optical and IR Telescope Instrumentation and Detectors, ed. M. Iye & A. F. Moorwood, Proc. SPIE, 4008, 623–631
Chebotarev, G. A. 1965, Sov. Astron., 8, 787
Clark, B. E., Bus, S. J., Rivkin, A. S., Shepard, M. K., & Shah, S. 2004, AJ, 128, 3070
de la Fuente Marcos, C., & de la Fuente Marcos, R. 2012, MNRAS, 427, 728
de la Fuente Marcos, C., & de la Fuente Marcos, R. 2015, MNRAS, 453, 1288
de la Fuente Marcos, R., & de la Fuente Marcos, C. 2018, Res. Notes Am. Astron. Soc., 2, 10
de la Fuente Marcos, C., de la Fuente Marcos, R., & Aarseth, S. J. 2018, MNRAS, 476, L1
Denneau, L., Jedicke, R., Grav, T., et al. 2013, PASP, 125, 357
De Prá, M. N., Pinilla-Alonso, N., Carvano, J. M., et al. 2018, Icarus, 311, 35
Fernández, J. A., Tancredi, G., Rickman, H., & Licandro, J. 1999, A&A, 352, 327
Fernández, J. A., Gallardo, T., & Brunini, A. 2004, Icarus, 172, 372
Fornasier, S., Clark, B. E., & Dotto, E. 2011, Icarus, 214, 131
Gibb, E. L., Mumma, M. J., Dello Russo, N., DiSanti, M. A., & Magee-Sauer, K. 2003, Icarus, 165, 391
Gilmore, A. C., Kilmartin, P. M., Meech, K. J., et al. 2018, Minor Planet Electronic Circulars, 2018-P86
Giorgini, J. D. 2015, IAU Gen. Assem., 22, 2256293
Granvik, M., Morbidelli, A., Jedicke, R., et al. 2018, Icarus, 312, 181
Howell, E. S., Rivkin, A. S., Vilas, F., et al. 2011, in EPSC-DPS Joint Meeting 2011, 637
Jewitt, D. 2015, AJ, 150, 201
Kaib, N. A., & Quinn, T. 2008, Icarus, 197, 221
Kaiser, N. 2004, in Ground-based Telescopes, ed. J. M. Oschmann, Jr., Proc. SPIE, 5489, 11–22
Królikowska, M., & Dybczyński, P. A. 2017, MNRAS, 472, 4634
Kulyk, I., Korsun, P., Rousselot, P., Afanasiev, V., & Ivanova, O. 2016, Icarus, 271, 314
Landolt, A. U. 1992, AJ, 104, 340
Levison, H. F., Duncan, M. J., Brasser, R., & Kaufmann, D. E. 2010, Science, 329, 187
Licandro, J., Tancredi, G., Lindgren, M., Rickman, H., & Hutton, R. G. 2000, Icarus, 147, 161
Licandro, J., Popescu, M., de León, J., et al. 2018, A&A, 618, A170
Luu, J. X., & Jewitt, D. C. 1996, AJ, 111, 499
Mazzotta Epifani, E., Perna, D., Di Fabrizio, L., et al. 2014, A&A, 561, A6
Meech, K. J., Yang, B., Kleyna, J., et al. 2016, Sci. Adv., 2, e1600038
Murray, C. D., & Dermott, S. F. 1999, Solar System Dynamics (Cambridge: Cambridge University Press)
Oort, J. H. 1950, Bull. Astron. Inst. Netherlands, 11, 91
Popescu, M., Birlan, M., & Nedelcu, D. A. 2012, A&A, 544, A130
Rivkin, A. S., Campins, H., Emery, J. P., et al. 2015, Astronomical Observations of Volatiles on Asteroids, ed. P. Michel, F. E. DeMeo, & W. F. Bottke, 65
S'arneczky, K., Weryk, R., Wainscoat, R., et al. 2018, Minor Planet Electronic Circulars, 2018-H21
Snodgrass, C., Fitzsimmons, A., Lowry, S. C., & Weissman, P. 2011, MNRAS, 414, 458
Stern, S. A., & Weissman, P. R. 2001, Nature, 409, 589
Tichy, M., Ticha, J., McMillan, R. S., et al. 2018, Minor Planet Electronic Circulars, 2018-F139